Local laser cooling of Yb:YLF to 110 K

Denis V. Seletskiy,[1,3,*] Seth D. Melgaard,[1] Richard I. Epstein,[1] Alberto Di Lieto,[2] Mauro Tonelli,[2] and Mansoor Sheik-Bahae[1]

[1]*Department of Physics and Astronomy, University of New Mexico,1919 Lomas Blvd. NE MSC074220, Albuquerque, NM 87131, USA*

[2]*DNEST Istituto Nanoscienze- CNR, Dipartimento di Fisica Università di Pisa, Largo B. Pontecorvo 3, 56127 Pisa, Italy*

[3]*Air Force Research Laboratory, Space Vehicles Directorate, Kirtland AFB, NM 87117, USA*

**d.seletskiy@gmail.com*

Abstract: Minimum achievable temperature of ~110 K is measured in a 5% doped Yb:YLF crystal at λ = 1020 nm, corresponding to E4-E5 resonance of Stark manifold. This measurement is in excellent agreement with the laser cooling model and was made possible by employing a novel and sensitive implementation of differential luminescence thermometry using balanced photo-detectors.

OCIS codes: (160.5690) Rare-earth-doped materials; (140.3320) Laser cooling.

References and links

1. P. Pringsheim, "Zwei bemerkungen uber den unterschied von lumineszenz- und temperaturstrahlung," Z. Phys. **57**(11-12), 739–746 (1929).
2. M. Sheik-Bahae and R. I. Epstein, "Optical refrigeration," Nat. Photonics **1**(12), 693–699 (2007).
3. M. Sheik-Bahae and R. I. Epstein, "Laser cooling of solids," Laser Photon. Rev. **3**(1-2), 67–84 (2009).
4. L. Landau, "On the thermodynamics of photoluminescence," J. Phys. (Moscow) **10**, 503–506 (1946).
5. R. I. Epstein, M. I. Buchwald, B. C. Edwards, T. R. Gosnell, and C. E. Mungan, "Observation of laser-induced fluorescent cooling of a solid," Nature **377**(6549), 500–503 (1995).
6. B. C. Edwards, J. E. Anderson, R. I. Epstein, G. L. Mills, and A. J. Mord, "Demonstration of a solid-state optical cooler: an approach to cryogenic refrigeration," J. Appl. Phys. **86**(11), 6489–6493 (1999).
7. G. Mills and A. Mord, "Performance modeling of optical refrigerators," Cryogenics **46**(2-3), 176–182 (2006).
8. S. R. Bowman, "Lasers without internal heat generation," IEEE J. Quantum Electron. **35**(1), 115–122 (1999).
9. R. Epstein and M. Sheik-Bahae, *Optical Refrigeration: Science and Applications of Laser Cooling of Solids*, 1st ed. (Wiley-VCH, 2009).
10. G. Nemova and R. Kashyap, "Laser cooling of solids," Rep. Prog. Phys. **73**(8), 086501 (2010).
11. D. V. Seletskiy, S. D. Melgaard, S. Bigotta, A. Di Lieto, M. Tonelli, and M. Sheik-Bahae, "Laser cooling of solids to cryogenic temperatures," Nat. Photonics **4**(3), 161–164 (2010).
12. D. V. Seletskiy, S. D. Melgaard, A. Di Lieto, M. Tonelli, and M. Sheik-Bahae, "Laser cooling of a semiconductor load to 165 K," Opt. Express **18**(17), 18061–18066 (2010), http://www.opticsinfobase.org/abstract.cfm?URI=oe-18-17-18061.
13. G. Lei, J. E. Anderson, M. I. Buchwald, B. C. Edwards, R. I. Epstein, M. T. Murtagh, and G. H. Sigel, "Spectroscopic evaluation of Yb^{3+}-doped glasses for optical refrigeration," IEEE J. Quantum Electron. **34**(10), 1839–1845 (1998).
14. M. P. Hehlen, R. I. Epstein, and H. Inoue, "Model of laser cooling in the Yb^{3+}-doped fluorozirconate glass ZBLAN," Phys. Rev. B **75**(14), 144302 (2007).
15. W. M. Patterson, M. Sheik-Bahae, R. I. Epstein, and M. P. Hehlen, "Model of laser-induced temperature changes in solid-state optical refrigerators," J. Appl. Phys. **107**(6), 063108 (2010).
16. G. Nemova and R. Kashyap, "Temperature distribution in laser-cooled rare-earth doped solid-state samples," J. Opt. Soc. Am. B **27**(12), 2460–2464 (2010).
17. C. E. Mungan, M. I. Buchwald, B. C. Edwards, R. I. Epstein, and T. R. Gosnell, "Internal laser cooling of Yb^{3+}-doped glass measured between 100 and 300 K," Appl. Phys. Lett. **71**(11), 1458–1460 (1997).
18. J. Fernández, A. Mendioroz, A. J. García, R. Balda, J. L. Adam, and M. A. Arriandiaga, "On the origin of anti-Stokes laser-induced cooling of Yb^{3+}-doped glass," Opt. Mater. **16**(1-2), 173–179 (2001).
19. M. P. Hasselbeck, M. Sheik-Bahae, and R. I. Epstein, "Effect of high carrier density on luminescence thermometry in semiconductors," Proc. SPIE **6461**, 646107 (2007).
20. R. L. Aggarwal, D. J. Ripin, J. R. Ochoa, and T. Y. Fan, "Measurement of thermo-optic properties of $Y_3Al_5O_{12}$, $Lu_3Al_5O_{12}$, $YAlO_3$, $LiYF_4$, $LiLuF_4$, BaY_2F_8, $KGd(WO_4)_2$, and $KY(WO_4)_2$ laser crystals in the 80–300 K temperature range," J. Appl. Phys. **98**(10), 103514 (2005).

#150822 - $15.00 USD Received 11 Jul 2011; revised 20 Aug 2011; accepted 22 Aug 2011; published 1 Sep 2011

21. Y. P. Varshni, "Band-to-band radiative recombination in groups IV, VI, and III-V semiconductors (I)," Phys. Status Solidi B **19**(2), 459–514 (1967).
22. C. E. Mungan, M. I. Buchwald, B. C. Edwards, R. I. Epstein, and T. R. Gosnell, "Laser cooling of a solid by 16 K starting from room temperature," Phys. Rev. Lett. **78**(6), 1030–1033 (1997).
23. B. Imangholi, M. Hasselbeck, D. Bender, C. Wang, M. Sheik-Bahae, R. Epstein, and S. Kurtz, "Differential luminescence thermometry in semiconductor laser cooling," Proc. SPIE **6115**, 61151C (2006).
24. D. V. Seletskiy, M. P. Hasselbeck, M. Sheik-Bahae, and R. I. Epstein, "Fast differential luminescence thermometry," Proc. SPIE **7228**, 72280K (2009).
25. W. M. Patterson, D. V. Seletskiy, M. Sheik-Bahae, R. I. Epstein, and M. P. Hehlen, "Measurement of solid-state optical refrigeration by two-band differential luminescence thermometry," J. Opt. Soc. Am. B **27**(3), 611–618 (2010).
26. N. Coluccelli, G. Galzerano, L. Bonelli, A. Di Lieto, M. Tonelli, and P. Laporta, "Diode-pumped passively mode-locked Yb:YLF laser," Opt. Express **16**(5), 2922–2927 (2008), http://www.opticsinfobase.org/oe/abstract.cfm?URI=oe-16-5-2922.
27. J. Thiede, J. Distel, S. R. Greenfield, and R. I. Epstein, "Cooling to 208 K by optical refrigeration," Appl. Phys. Lett. **86**(15), 154107 (2005).
28. D. V. Seletskiy, R. I. Epstein, and M. Sheik-Bahae, "Progress toward sub-100 Kelvin operation of an optical cryocooler," Proc. SPIE **7951**, 795103 (2011).

1. Introduction

Optical refrigeration or laser cooling of solids is based on anti-Stokes fluorescence [1]. When the laser excitation wavelength is above mean emission wavelength (λ_f) of a given transition, the subsequent fluorescence requires phonon absorption in order to establish quasi equilibrium. The efficient escape of the upconverted fluorescence would then carry heat out of the material resulting in net cooling [2–4].

Laser cooling of a solid was first demonstrated in a Yb-doped glass by Epstein *et. al.* in 1995 [5]. Soon after this report, many innovative applications such as an all-solid-state optical cryocooler [6,7] and radiationally-balanced laser [8] were proposed. To date, laser cooling has been observed in a wide variety of glass and crystalline hosts, doped with trivalent rare-earth ions of Yb, Tm and Er (for a recent broad literature review see for e.g [3,9,10]). Excitation near the Stark-manifold E4-E5 resonance of a Yb^{3+}-doped $LiYF_4$ (Yb:YLF) crystal has recently led to bulk cooling from room temperature to 155 K [11]. Subsequently, the same system was used to cool a semiconductor (GaAs) payload to 165 K [11,12]. The above results were limited by low pump power and more importantly by the shortest wavelength of the tunable pump laser (Yb:YAG, 1023-1040 nm). Our laser cooling model predicted that the minimum achievable temperature (MAT) of ~115 K should be possible if the excitation is tuned exactly to the E4-E5 Stark resonance of Yb^{3+} at ~1020 nm [11]. In this paper we report on the experimental validation of the model by conducting spectroscopic measurements of the cooling efficiency of the Yb:YLF sample. The verification of local cooling to 110 ± 5 K, as reported in Section 4 of this paper, represents a major milestone in optical refrigeration as it demonstrates cooling below 123K (–150 C), designated by NIST as the onset of cryogenics. These measurements were made possible utilizing a novel and sensitive pump-probe technique of two-band differential spectral metrology (2B-DSM), which probes local temperature change directly. This is in contrast to a more popular photo-thermal deflection method where various competing contributions complicate signal interpretation.

2. Modeling of the cooling efficiency

The cooling efficiency, defined as the ratio of the cooling power (P_{cool}) to the absorbed laser power (P_{abs}), is given by [2]:

$$\eta_c(\lambda,T)=\frac{P_{cool}}{P_{abs}}=\eta_{ext}\left[\frac{1}{1+\alpha_b/\alpha(\lambda,T)}\right]\frac{\lambda}{\lambda_f(T)}-1, \qquad (1)$$

where η_{ext} is the external quantum efficiency (EQE) defined as the fraction of excited ions that lead to a fluorescence photon exiting the host material. High η_{ext} (> 99%) is known for rare-

#150822 - $15.00 USD Received 11 Jul 2011; revised 20 Aug 2011; accepted 22 Aug 2011; published 1 Sep 2011

earth ions in low phonon energy hosts (such as fluorides), making them ideal candidates for laser cooling. Furthermore, it is generally expected (and experimentally verified) that η_{ext} is rather temperature independent [13]. The cooling transition is characterized by an absorption coefficient $\alpha(\lambda,T)$ and mean fluorescence wavelength $\lambda_f\ (T)$ (taking into account effect of luminescence trapping and re-absorption), while α_b describes the background parasitic absorption. In the sign convention adopted here, negative values of the cooling efficiency correspond to heating. The term in the square brackets of Eq. (1) corresponds to the fraction of the total absorbed photons that lead to an excitation of the cooling transition in the rare-earth ion (e.g. $^2F_{7/2}$ – $^2F_{5/2}$ transition in Yb^{3+}), and therefore is referred to as absorption efficiency η_{abs}. The product $\eta_{ext}\eta_{abs}$ can therefore be interpreted as the efficiency (or probability) of converting an absorbed photon to an escaped fluorescence photon. The background absorption α_b most likely originates from unwanted contamination during growth, particularly from transition metals such as copper and iron, similar to glass hosts [14]. In the cooling model, α_b is also taken to be temperature independent, and broadband (i.e. independent of wavelength) within the spectral region of the cooling transition [14].

Due to Boltzmann distribution of populations in both ground and excited states, as well as the vibrationally broadened levels in the Stark manifolds, both λ_f and α are functions of lattice temperature. Upon lowering of temperature, the cooling efficiency in the cooling region (for fixed λ and α_b) decreases due to diminishing resonant absorption α and red-shift of λ_f, until it becomes negative, corresponding to overall heating. The temperature corresponding to the transition point from cooling to heating is the minimum achievable temperature (MAT) at that wavelength, i.e. MAT(λ). For a given material, a minimum temperature T_{min} of the MAT spectrum (i.e. a *global* MAT) is defined as the minimum temperature T_{min} at which $\eta_c(\lambda,T_{min}) = 0$ or simply the temperature at which $\partial MAT(\lambda)/\partial\lambda = 0$. Prediction of MAT($\lambda$) and hence T_{min} of a given material requires knowledge of $\eta_c(\lambda,T)$ which in turn necessitates that its four constituents $\alpha(\lambda,T)$, $\lambda_f\ (T)$, η_{ext} and α_b be known. As will be detailed in Section 4, we experimentally determined these four parameters for a 5% Yb:YLF crystal for the excitation in the E||c orientation. Figure 1 shows thus constructed temperature-dependent spectra of the cooling efficiency. A minimum achievable temperature (MAT) of ~115 K is predicted to occur at ~1020 nm, corresponding to the transition between E4 and E5 levels of the $^2F_{7/2}$ – $^2F_{5/2}$ Stark manifold of Yb^{3+}.

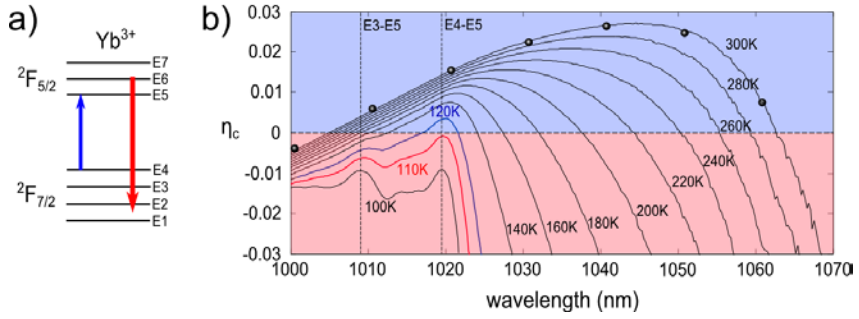

Fig. 1. (a) Schematic of the Stark manifold associated with $^2F_{7/2}$ – $^2F_{5/2}$ transition in Yb^{3+} ion; (b) Calculated temperature-dependent spectra of the cooling efficiency η_c of a 5% Yb^{3+}:YLF_4 crystal for E||c orientation with η_{ext} = 0.995 ± 0.001 and α_b = (4.0 ± 0.2) × 10^{-4} cm^{-1}, as determined from the fit of the experimental data at 300 K (black circles). Transition from cooling to heating-only occurs between 120 K (blue line) and 110 K (red line), bracketing a minimum achievable temperature at ~115 K near 1020 nm, corresponding to E4-E5 Stark manifold transition of Yb^{3+}. Resonant feature corresponding to E3-E5 transition is also evident at ~1010 nm, but does not lead to cooling efficiency enhancement for given values of η_{ext} and α_b.

#150822 - $15.00 USD Received 11 Jul 2011; revised 20 Aug 2011; accepted 22 Aug 2011; published 1 Sep 2011

3. Two-band differential spectral metrology (2B-DSM)

In order to directly verify the cooling efficiency spectra (Fig. 1) and in particular MAT(λ), we set out to perform a pump-probe experiment to measure "local" laser-induced temperature change as a function of global (bulk) temperature of the sample. For this, the bulk temperature of the Yb:YLF is varied by means of a cryostat through an efficient thermal contact of the crystal with the cryostat's coldfinger. In this arrangement, laser cooling occurs only within a limited spatio-temporal (i.e. local) window. That is, the laser-irradiated spot initially cools before reversing, as the heat from fluorescence absorption at the surface contacts diffuses back into the cooled region. While the spatial variation of the temperature field has been addressed previously [15,16], the temporal dependence pointed out here is due to the particular geometry of the experimental setup, i.e. the presence of good thermal contact of the crystal with the coldfinger. The duration of this local cooling becomes shorter for crystals with relatively high thermal conductivity such as YLF (as compared with glasses). This restriction motivated us to develop a novel and highly sensitive fast fluorescence-based temperature measurement technique. This technique is described in the current section while its application to determination of MAT(λ) is discussed in Section 4 of the paper.

Before we describe our technique, we also should note that a pump-probe arrangement to detect local temperature (i.e. spatio-temporally resolved temperature in the region interrogated by the probe beam) through an induced refractive index change (photo-thermal deflection spectroscopy PTDS) was employed in the past to perform room temperature [5,13,17,18] as well as cryogenic [13,17] cooling measurements in Yb-glasses. However, techniques relying on a refractive index measurement (e.g. PTDS) need to separate the thermal contribution to the index change from the accompanying contribution caused by pump-induced population changes in both ground and excited states [19]. We note that such separation, in principle, cannot be achieved by wavelength selection of the probe alone, since pump-induced absorption change leads to a refractive index change at all wavelengths as per Kramers-Kronig relations. This complication in turn necessitates a lateral displacement of the pump and probe beams, since heat diffuses outward while the population excitation remains local. Thus the need for optimal focusing geometries for both pump and probe beams and their optimal lateral displacement (in general both are temperature dependent through thermal diffusivity of a medium, e.g. YLF [20]) complicate the measurements and can even lead to erroneous results, especially at low temperatures.

The fluorescence spectrum of the solid can also be used to infer its temperature with high sensitivity [11,21–23]. In this situation, carrier density effects are alleviated by maintaining probe beam at constant power and therefore no displacement between pump and probe beams is required. Sensitivity is also increased using difference luminescence thermometry (DLT), obtained upon subtraction of the acquired spectra at two different temperatures [11,22,23]. While highly sensitive, the speed of this technique is limited by the spectrometer (CCD) readout time, which is typically in the tens of milliseconds range for the standard devices. In addition, sensitivity of the measurement is degraded from inherent CCD dark counts and readout noise.

To circumvent these limitations, we perform a dual-band spectral differencing via a balanced amplified photodetector (BAPD, for e.g. a bi-cell PD) directly in the spectral domain [24]. Due to the large electronic bandwidth and high common-mode-rejection of these detectors, a fast and shot-noise-limited performance can be obtained relatively easily. Fluorescence spectrum can be sampled for example by means of a monochromator (MC) [24], color filters [25], or any other spectrally selective components. Color filters for example are more suitable for resolving a temperature-induced spectral linewidth change of a fixed transition frequency (e.g. Yb^{3+} ion), while the MC offers a continuously-tunable choice for the temperature-dependent transition frequencies, such as bandgap of a semiconductor (e.g. GaAs). We have termed this technique *2-band differential spectral metrology* (2B-DSM).

#150822 - $15.00 USD Received 11 Jul 2011; revised 20 Aug 2011; accepted 22 Aug 2011; published 1 Sep 2011

In this work we exploit the temperature-dependent bandgap shift of a GaAs/GaInP double heterostructure (GaAs DHS), attached to the Yb:YLF sample [12] as a means of the 2B-DSM probe. To this end, a portion of the luminescence spectrum of GaAs $S(\lambda)$ is interrogated at the exit slit of a monochromator by the BAPD, such that the resulting signal (V) is [24]:

$$V(\lambda_0, T_0) \propto S(\lambda_0 + \Delta\lambda, T_0) - S(\lambda_0 - \Delta\lambda, T_0) \propto \left(\left. \frac{\partial S}{\partial \lambda} \right|_{\lambda_0, T_0} \right), \tag{2}$$

where T_0 is the GaAs temperature, λ_0 is the center wavelength of the spectral region within the exit slit of width $2\Delta\lambda$. The spectral derivative approximation assumes that $2\Delta\lambda$ is still narrower than any spectral feature of the luminescence lineshape $S(\lambda)$. For small temperature change (ΔT) about the initial T_0, the V signal (up to the first order) is then given by:

$$V(\Delta T, \lambda_0) \propto \left(\left. \frac{\partial S}{\partial \lambda} \right|_{\lambda_0, T_0} \right) + \left. \frac{\partial}{\partial T} \left(\left. \frac{\partial S}{\partial \lambda} \right|_{\lambda_0} \right) \right|_{T_0} \Delta T + \mathrm{O}\left[(\Delta T)^2 \right]. \tag{3}$$

By the appropriate choice of λ_0, temperature-independent offset [first term on the right hand side of Eq. (3)] can be nullified, such that the signal V (in both magnitude and sign) is background-free and linearly proportional to the temperature change ΔT. We note that even if the derivative approximation in above expressions cannot be made, spectral shift of the luminescence as measured by the differential V signal can still be calibrated to be proportional to the temperature change.

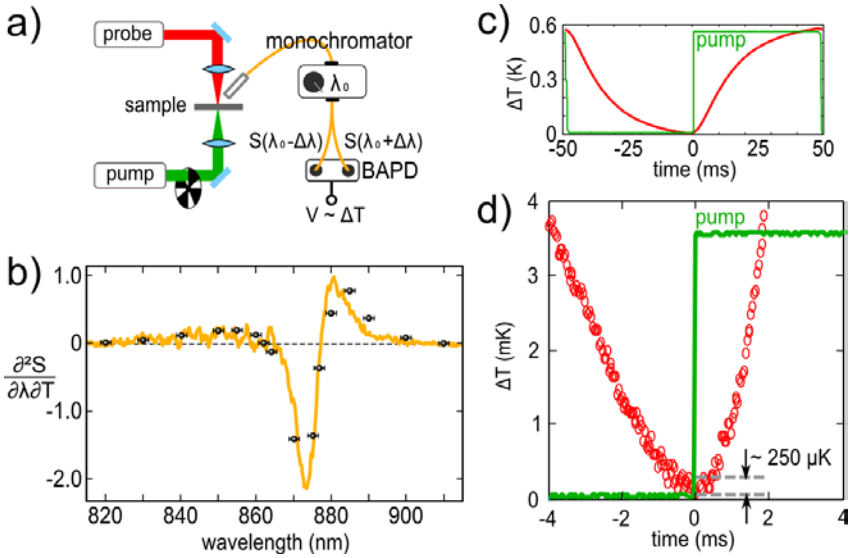

Fig. 2. (a) Schematic of the pump-probe setup, BAPD – balanced amplified photodiode, signal (V) is proportional to the change of temperature (ΔT); (b) Normalized calculated and box-car averaged thermo-spectral derivative (orange line) of a GaAs DHS evaluated at λ_0 and T_0 = 300K is plotted versus λ_0 together with the normalized magnitude of a measured differential modulated signal (V) (black circles); (c) Modulated pump (green) and temperature (red), as obtained from the probe signal when GaAs semiconductor is excited by 50 mW of 532nm pump and monitored at λ_0 ~870 nm; (d) Magnification of the panel (c) around t = 0 point; resolution of ~250 μK is demonstrated after 10,000 waveform averages on an oscilloscope.

First we perform stand-alone experiment on GaAs/InGaP double heterostructure to demonstrate the sensitivity of the 2B-DSM technique. Here, a 500 μm thick GaAs DHS is excited from opposite sides by a pump laser (50 mW at 532 nm, modulated at 10 Hz) and a 650 nm probe laser, focused to their respective spot sizes of ~200μm and 150μm [Fig. 2(a)]. Probe-induced luminescence is collected by a 600 μm diameter optical fiber and routed into

#150822 - $15.00 USD Received 11 Jul 2011; revised 20 Aug 2011; accepted 22 Aug 2011; published 1 Sep 2011

the entrance slit of a scanning MC. Closely spaced and properly oriented cores of two optical fibers at the exit slit of the MC pick up the respective components of the spectrally-dispersed luminescence signal and couple them into the input ports of the BAPD (New Focus Model 2307). Modulated pump induces a time-varying differential signal, which is pre-amplified and then averaged on an oscilloscope [Fig. 2(c)]. Complimentary to the differential signals, spectrometer (Ocean Optics HR4000 with 10μm slits) is used to measure luminescence spectra of GaAs DHS with and without modulated pump. These additional measurements allowed us to calibrate pump-induced heating of the sample (through a Varshni relation [21]) as well as allowed for a comparison of the differential signals with that of the predicted behavior in Eq. (3). Figure 2(b) shows room-temperature calculated spectrum of $\partial^2 S / \partial\lambda\partial T\big|_{\lambda_0,T_0}$, performed on a box-car averaged spectra $S(\lambda)$, with a box size corresponding to $\Delta\lambda$ of 5 nm of the MC. Maximum signal deviation occurs for $h\nu_0 \sim E_g$, the bandgap energy of the GaAs DHS ($\lambda_0 = c/\nu_0 \sim 870$ nm). Magnitude of the time-dependent component of the differential signals is plotted on the same axes for various grating positions (λ_0). A very good agreement is observed, verifying Eq. (3) and in particular the linear dependence of the differential signal (V) on the small ΔT, induced by the pump beam. An uncertainty in abscissa coordinate of the 2B-DSM signal is mainly due to the backlash of the screw-controlled grating position of our compact mini-MC (Optometrics). Small systematic differences between calculated and measured values of the derivative spectra are attributed to spectral response differences of the spectrometer CCD and each of the balanced detectors, together with possible higher order contributions (neglected terms in Eq. (3).

To identify the temperature resolution of the technique, we average 10,000 time-resolved oscilloscope traces of the probe signal monitored at $\lambda_0 = 870$ nm, and converted to temperature by means of a Varshni formula [21]. For a 50 mW pump laser, heating of the heat-sunk GaAs DHS by 0.6 degrees was deduced [Fig. 2(c)]. A close-up view at the early-time probe signal reveals temperature resolution of ~250 μK over on a sub-millisecond time scale [Fig. 2(d)]. This performance allows for a sensitive determination of the MAT(λ) spectrum.

4. Spectroscopy of the minimum achievable temperature (MAT)

The spectroscopy of the cooling efficiency is performed on a high-purity, Czochralski-grown 5%-doped Yb:YLF crystal of dimensions 3 × 3 × 9 mm^3 [11,12,26], excited in the $E||c$ orientation along the long axis. As was mentioned above, for modeling of the cooling efficiency (Fig. 1), we experimentally obtained quantities $\alpha(\lambda,T)$, $\lambda_f(T)$, η_{ext} and α_b. To this end, temperature-dependent polarized and unpolarized instrument-response-corrected fluorescence spectra of the Yb:YLF sample were obtained by placing the crystal inside a cryostat. Mean fluorescence wavelength $\lambda_f(T)$ was calculated by taking a first moment of the unpolarized fluorescence spectra, while resonant absorption spectra $\alpha(\lambda,T)$ were obtained from the reciprocity analysis of the polarized emission.

To obtain external quantum efficiency and background absorption values, an additional experiment was performed at room temperature, where sample was excited by a tunable (950nm-1080nm, 1.3-1.8 W) CW Ti:Sapphire laser and crystal temperature was monitored using a bolometric thermal camera. The obtained temperature change, normalized by the absorbed power, is linearly proportional to the cooling efficiency. We fit the data (Fig. 1, black circles) to the cooling efficiency relation [Eq. (1)] to extract $\eta_{ext} = 0.995 \pm 0.001$ and $\alpha_b = (4.0 \pm 0.2) \times 10^{-4}$ cm^{-1}.

Next, we discuss the application of a 2B-DSM technique to test modeling predictions in Fig. 1. The tunable pump (Ti:Sapphire laser) excites Yb:YLF sample held at variable starting temperatures (T_0) by means of a contact with a coldfinger of a liquid nitrogen filled cryostat [Fig. 3(a)], which uses a thermal impedance displacer together with a built-in heating element to allow for a potential set temperature in the range of 80 – 350 K. Luminescence of GaAs/GaInP DHS, attached to the side of the Yb:YLF, is excited by a CW probe beam (650

#150822 - $15.00 USD Received 11 Jul 2011; revised 20 Aug 2011; accepted 22 Aug 2011; published 1 Sep 2011

nm, 20 mW) and collimated by a lens (N.A. = 0.42) after the cryostat viewport. Another lens (N.A. = 0.22) is used to refocus the luminescence signal into a NA-matched optical fiber (600 μm core), which in turn is coupled into an entrance port of a mini-monochromator for differential detection (as detailed in the previous section).

Pump-induced temperature change ΔT, corresponding to laser cooling, is expected to be small and fast, following initial pump turn on. This is because at times larger than the thermal transport time across the crystal, its temperature is dictated not by the pump laser but by the heat generated by fluorescence absorption at the coldfinger, diffusing from the coldfinger contacts back into the excitation volume. Fast measurement of the DHS temperature is thus capable of separating the initial local temperature $T_0 - \Delta T$ (due to laser cooling process) from the background heat at the later times. An additional thermal capacitance has been added at the contact points of the crystal with the coldfinger surfaces (150 μm thick BK7 plates) in order to increase the transport time of the background heat and thus increase the time window over which the local temperature change can be observed. Finally, pump is traversing the Yb:YLF parallel and very near the surface with the attached DHS [Fig. 3(a)], thus minimizing thermal transport time of the laser cooling signal, as detected by the bandgap shift of the DHS.

Figure 3(b) shows time traces of the 2B-DSM signals (spectral derivative, see Section 3) from Yb:YLF/GaAs at room temperature. When pump is tuned below (980 nm) and above (1020 nm) the mean luminescence wavelength (~1000 nm), clear phase-shift of the time traces is evident. For a given excitation wavelength, the transition temperature between local cooling and heating determines the minimum achievable temperature (MAT) for that excitation condition. For each excitation wavelength, we vary the bulk sample temperature (T_0) via the cryostat, until transition from cooling to heating is observed, corresponding to a sign change of the measured ΔT [Fig. 3(b)]. These transition temperatures are then plotted in Fig. 3(c), superimposed on top of a contour plot of the cooling efficiency spectra, as calculated from Eq. (1) and also represented in Fig. 1. The red color corresponds to heating regions, while the blue area is consistent with cooling. The line separating these regions defines the MAT(λ).

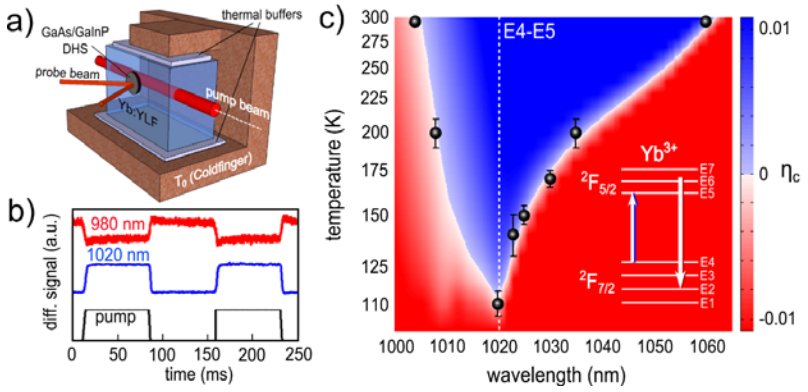

Fig. 3. (a) Schematic of the experimental arrangement: Yb:YLF is clamped by the coldfinger arrangement that is held at T_0; local temperature change due to the pump beam is detected via luminescence from a GaAs/InGaP double heterostructure, excited in turn by the probe laser. Thermal buffers serve to maximize local signal, while maintaining Yb:YLF temperature near the T_0 setpoint; (b) Normalized and vertically-shifted time traces of the spectral derivative signals, showing a clear phase-reversal between the heating (980 nm) and cooling (1020 nm) excitations at room temperature; (c) comparison of the contour plot of the calculated cooling efficiency with the measurement (circles) of the wavelength-dependent minimum achievable temperature MAT(λ), separating cooling (blue) and heating (red) regions, cooling to 110 ± 5 K at ~1020 nm is demonstrated; inset shows energy diagram (not to scale) of the Yb^{3+} Stark level manifold.

We point out that MAT condition predicted from the model is in a very good quantitative agreement with the measurements [Fig. 3(c)], verifying both the narrowing of cooling window

#150822 - $15.00 USD Received 11 Jul 2011; revised 20 Aug 2011; accepted 22 Aug 2011; published 1 Sep 2011

at lower temperatures and its convergence to the wavelength of 1020 nm, corresponding to the E4-E5 Stark manifold transition [11]. In particular, a measured MAT(1020 nm) = 110 ± 5 K is in excellent agreement with the model, within the current experimental uncertainty, as determined by the experimenters' choice of the temperature step in T_0. This temperature is below the NIST-defined cryogenic onset of 123 K and corresponds to the lowest temperature obtained by means of optical refrigeration. Other researchers have also reported or inferred observation of local cooling below 110 K in ytterbium-doped glasses [13,17,18] using photo-thermal deflection spectroscopy. As discussed above, however, photo-thermal deflection measurements are difficult to interpret unambiguously, especially near the MAT where the signal to noise is small. The present results are not plagued by these ambiguities. In particular we have demonstrated quantitative agreement between the empirical modeling, local measurements and the earlier reported bulk cooling of Yb:YLF to 155 K at 1023 nm [11]. Demonstrated success of the cooling efficiency model also allows us to more confidently estimate MAT of a typical Yb:ZBLAN (fluorozirconate glass host) to be ~180 K. This value is warmer than MAT of Yb:YLF due to large inhomogeneous broadening of the Stark-manifold levels in glass host, together with smaller allowable Yb^{3+} doping concentration (than in YLF) and comparable background absorption values [27]. Furthermore, previous bulk cooling measurements in Yb:ZBLAN to 208 K at 1026 nm [27] are also consistent with the estimates from the current cooling efficiency model.

Finally, we note that this verification of the model also supports the built-in assumptions, namely wavelength- and temperature-independence of the background absorption coefficient. This, in turn, suggests transition metal impurities as the likely source of the parasitic background absorption in YLF, in similarity to the glass hosts [14]. Identifying these impurities directly is a formidable task, as their estimated concentrations are well below part per million levels. The obvious incentive however is that temperatures below 100 K and even approaching 77 K are possible upon an order-of-magnitude improvement of the present crystal purity [28].

5. Conclusion

Measurement of a spectrum of the minimum achievable temperatures in a 5%-doped Yb:YLF crystal is reported using a novel pump-probe technique. The obtained spectrum and in particular its minimum of 110 ± 5 K at E4-E5 Stark manifold resonance of Yb^{3+}, are in excellent agreement with the model predictions. This temperature corresponds to the coldest (local) temperature obtained by optical refrigeration to date and is below the NIST-defined onset of cryogenics at 123 K.

These results were possible via a non-contact and highly sensitive 2-band differential spectral metrology (2B-DSM, patent pending) pump-probe technique. In particular we have demonstrated temperature resolution of ~250 μK on a sub-millisecond time scale. The speed and sensitivity of this technique have allowed us to resolve the initial (local) temperature dynamics in the Yb:YLF crystal. This technique is general and we envision applications in derivative spectroscopic methods as well as flow cytometry to name few examples.

While this work verifies the predicted potential of the current Yb:YLF sample to cool to ~110 K, bulk cooling from ambient to this temperature using a high power laser at ~1020 nm remains to be demonstrated.

Acknowledgments

We thank Dr. Markus Hehlen for useful discussions. We also thank Mr. Chengao Wang for GaAs sample preparation and Dr. Michael Hasselbeck for his assistance with LabView software. This work was supported by an AFOSR Multi-University Research Initiative Grant No. FA9550-04-1-0356 entitled Consortium for Laser Cooling in Solids, and a DARPA seedling grant. Research in part was performed while DVS held a National Research Council Research Associateship Award at Air Force Research Laboratory.

#150822 - $15.00 USD Received 11 Jul 2011; revised 20 Aug 2011; accepted 22 Aug 2011; published 1 Sep 2011